

On significance of VLBI/*Gaia* position offsets

L. Petrov^{1★} and Y. Y. Kovalev^{2,3★}

¹*Astrogeo Center, 7312 Sportsman Dr., Falls Church, VA 22043, USA*

²*Astro Space Center of Lebedev Physical Institute, Profsoyuznaya 84/32, 117997 Moscow, Russia*

³*Max-Planck-Institut für Radioastronomie, Auf dem Hügel 69, D-53121 Bonn, Germany*

Accepted 2017 January 2. Received 2016 December 15; in original form 2016 November 6

ABSTRACT

We have cross matched the *Gaia* Data Release 1 secondary data set that contains positions of 1.14 billion objects against the most complete to date catalogue of very long baseline interferometry (VLBI) positions of 11.4 thousand sources, almost exclusively active galactic nuclei. We found 6064 matches, i.e. 53 per cent radio objects. The median uncertainty of VLBI positions is a factor of 4 smaller than the median uncertainties of their optical counterparts. Our analysis shows that the distribution of normalized arc lengths significantly deviates from Rayleigh shape with an excess of objects with small normalized arc lengths and with a number of outliers. We found that 6 per cent matches have radio-optical offsets significant at 99 per cent confidence level. Therefore, we conclude there exists a population of objects with genuine offsets between centroids of radio and optical emission.

Key words: galaxies: active – radio continuum: galaxies.

1 INTRODUCTION

The secondary data set of the first release of astrometric data from the European Space Agency mission *Gaia* contains positions of 1.14 billion objects (Lindegren et al. 2016). Of them, the vast majority are stars, though over one hundred thousands of extragalactic objects, namely active galactic nuclei (AGN), were also included in the catalogue. The position uncertainty of the *Gaia* DR1 secondary data set, 2.3 mas median, is two orders of magnitude higher than the uncertainty of previous large all-sky catalogue in optical wavelengths NOMAD (Zacharias et al. 2004) of 1.17 billion objects. The only technique that can determine positions of target sources with comparable accuracy is very long baseline interferometry (VLBI). The first insight on comparison of *Gaia* and VLBI position catalogues can be found in Mignard et al. (2016), who found that the overall agreement between the optical and radio positions is excellent, though a small number of sources (~6 per cent) show significant offsets.

In this Letter, we make our own comparison of *Gaia* and VLBI positions beyond that reported in Mignard et al. (2016). Several factors motivated us. First, the authors of the cited paper ran their comparison against the auxiliary *Gaia* quasar solution for some 135 000 quasars. This solution is not yet published in full, and only positions of 2 per cent of the objects were reported. The question of how results of the comparison against this auxiliary solution are representative to the main solution of one billion objects remained opened.

Secondly, Mignard et al. (2016) used the ICRF2 catalogue (Fey et al. 2015) for their comparison. This catalogue assembled in 2008–2009 represented the state of the art by 2008 and comprised of sources observed in geodetic programs (Ma et al. 1998; Petrov et al. 2009) and six Very Long Baseline Array (VLBA) Calibrator Surveys (Beasley et al. 2002; Fomalont et al. 2003; Petrov et al. 2005, 2006; Kovalev et al. 2007; Petrov et al. 2008). Since then there was an explosive growth of absolute astrometry VLBI programs: VLBA and European VLBI network Galactic plane surveys (Petrov et al. 2011a; Petrov 2012); VLBA Imaging and Polarimetry Survey (VIPS) (Petrov & Taylor 2011); Australian Long Baseline Calibrator Survey (LCS) (Petrov et al. 2011b); the VLBA Calibrator Search for the BeSSel Survey (Immer et al. 2011); the VLBA survey of bright 2MASS galaxies (V2M) (Condon et al. 2017); the VLBA+EVN survey of optically bright extragalactic radio sources (OBRS–1, OBRS–2) (Petrov 2011, 2013); the second epoch VLBA calibrator survey observations (VCS-ii), (Gordon et al. 2016). Besides, there are a number of ongoing surveys: the VLBI Ecliptic Plane Survey (VEPS) (Shu et al. 2016), the wide-band VCS7, VCS8 and VCS9 surveys (Petrov 2016), and the VLBI survey of *Fermi* detected γ -ray sources (Schinzel et al. 2015). By 2016 September 14, the date of *Gaia* DR1 release, the total number of sources with positions determined with absolute astrometry using VLBI reached 11 444, a factor of 3.5 increase with respect to the ICRF2.

Thirdly, the analysis of Mignard et al. (2016) showed that there exist sources with significant radio-optical offsets. Early comparisons of source positions from VLBI and ground optical observations prompted Zacharias & Zacharias (2014) and Orosz & Frey (2013) to surmise that there is a population of radio-optical offset objects with position differences in a range of 10–100 mas. Large offsets can occur either due to unaccounted errors in optical

* E-mail: Leonid.Petrov@lpetrov.net (LP); yyk@asc.rssi.ru (YYK)

positions or a gross oversight in deriving VLBI coordinates, or due to an offset between the centroids of radio and optic emission. We call latter objects genuine radio-optical offset (thereafter, GROO) sources. An increase in the accuracy of the optical positions by two orders magnitude allows us to re-examine the question of the GROO population existence. If such a population exists, it poses a challenge to explain significant radio-optical offsets.

2 ASSOCIATION OF VLBI AND *Gaia* OBJECTS

Our study is based on the analysis of the catalogue called *Gaia* DR1 secondary data set. We used for our work positions, their uncertainties, correlations between right ascension and declination for 1 142 679 769 objects. We did not analyse *Gaia* data and took the catalogue as it is. On the other hand, we reprocessed all publicly available VLBI data listed in the previous section from the level of visibilities using VLBI data analysis software PIMA¹. Detailed description of the analysis strategy and comparison with the methods adopted in the past and those used for processing the data can be found in Petrov et al. (2011a). An important conclusion of that comparison was that it does not introduce systematic differences at least above the 0.2 mas level with respect to the old processing pipeline. The specific VLBI catalogue used in our study is rfc_2016c². It is based on all geodesy and absolute astrometry VLBI data since 1980 April through 2016 July, including all observations used for deriving the ICRF2 catalogue and those that became publicly available since 2008.

At the first step, we identified all *Gaia* sources that lie within 5 arcsec of VLBI objects and found 6954 preliminary matches. We should note the source density of *Gaia* DR1 is substantially heterogeneous (see fig. 9 in Lindegren et al. (2016): the density in the Galactic plane exceeds by two order of magnitude the density near the Galactic poles. To take into account variations of *Gaia* spatial source density, we counted *Gaia* sources on the regular 0.25×0.25 grid and normalized the count to the number of sources per steradian. Then for a given match, we computed the probability of false association (PFA) as the product of local *Gaia* source density and the area πd^2 , where $d = L_{VG} + 3 \max(\sigma_{g, \text{maj}}, \sigma_{v, \text{maj}})$, L_{VG} is the arc length VLBI/*Gaia*, $\sigma_{g, \text{maj}}$ and $\sigma_{v, \text{maj}}$ are semimajor error ellipse axes for *Gaia* and VLBI, respectively. This conservative estimate of the PFA takes into account possible errors that affect d and represents rather its upper limit. The total number of matches with the PFA less than 2×10^{-4} is 6064. Of them, nine are radio stars. We have excluded them from further analysis. According to the selected PFA cut-off criterion, the mathematical expectation of the number of spurious matches within our conservative sample is 0.03, i.e. less than one object. We certainly missed some real matches, but for the purpose of this Letter it is more important to prevent false matches in the sample.

In total, 53 per cent VLBI sources are associated with a *Gaia* counterpart. The fraction of VLBI/*Gaia* matches monotonically decreases with a decrease of radio flux density: from 0.8 for sources with flux density >1 Jy at 8 GHz to 0.4 for sources with flux density in range of 10–40 mJy – see Fig. 1. At the same time, the diagram flux density versus G magnitude does not show any correlation. Since according to Lindegren et al. (2016), the *Gaia* DR1 is not complete in any sense, we defer analysis why the share of VLBI/*Gaia* matches drops with a decrease of flux density till

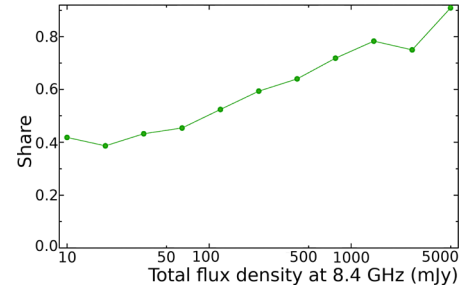


Figure 1. The fraction of sources found in *Gaia* catalogue as a function of the total flux density at 8.4 GHz integrated over parsec-scale image in logarithmic scale.

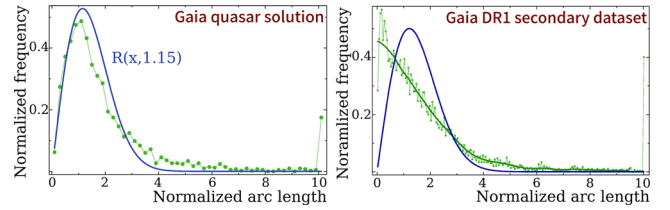


Figure 2. Left: normalized arc length among the 2080 VLBI/*Gaia* matches of QS sub-sample from the *Gaia* quasar solution. The continuous blue line shows the best-fitting Rayleigh distribution with parameter $\sigma = 1.15$. Right: the distribution of normalized arc lengths among all 6055 matches from the *Gaia* DR1 solution. The thick blue line is the best fit to the Rayleigh distribution, which is certainly inadequate.

deep optical surveys, such as Pan-STARRS that is expected to be complete at least to 23 mag, will become available.

3 ANALYSIS OF VLBI/*Gaia* ARC LENGTHS

We computed the normalized arc lengths between VLBI positions from rfc_2016c solution and the *Gaia* auxiliary quasar solution. We normalize the arc lengths exactly the same way as Mignard et al. (2016):

$$q^2 = (d_\alpha, d_\delta) \cdot \begin{pmatrix} \sigma_{g,\alpha}^2 + \sigma_{v,\alpha}^2 & \text{Cov}(\alpha, \delta)_g + \text{Cov}(\alpha, \delta)_v \\ \text{Cov}(\alpha, \delta)_g + \text{Cov}(\alpha, \delta)_v & \sigma_{g,\delta}^2 + \sigma_{v,\delta}^2 \end{pmatrix}^{-1} (d_\alpha, d_\delta)^\top$$

where d_α, d_δ are VLBI/*Gaia* offsets in right ascension multiplied by factor $\cos \delta$ and declination, $\sigma_{g,\alpha}$ and $\sigma_{v,\alpha}$ are reported uncertainty in right ascensions (including the factor $\cos \delta$) of *Gaia* and VLBI positions, respectively, and $\sigma_{g,\alpha}, \sigma_{v,\alpha}$ are reported uncertainties in declinations.

The distribution of normalized arc lengths, square root of q^2 of that sub-sample denoted as QS is shown in the left part of Fig. 2. The distribution is very close to that shown in fig. 8 of Mignard et al. (2016) based on analysis of the auxiliary *Gaia* quasar solution and the ICRF2 catalogue. The blue line in the left part of Fig. 2 shows the Rayleigh distribution³ with $\sigma = 1.15$ that fit best to the histogram that again is very close to the value 1.11 reported by Mignard et al. (2016). This confirms our previous assertion that the differences in positions of sources common for the ICRF2 and rfc_2016c catalogues are not essential for this study.

¹ See <http://astrogeo.org/pima>.

² Available online at <http://astrogeo.org/rfc>.

³ If position errors over each coordinate obey the Gaussian distribution, then the normalized arc lengths obey the Rayleigh distribution.

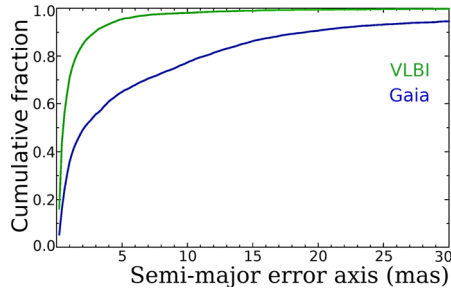


Figure 3. Cumulative distribution function of semimajor error axes $P(\sigma_{\text{maj}} < a)$: green (upper) curve for VLBI and blue (low) curve for *Gaia*.

However, the distribution of normalized arc lengths between positions from the *Gaia* DR1 secondary solution and VLBI is remarkably different (right part of Fig. 2). It is definitely very far from the Rayleigh distribution.

The normalized arc lengths depend on both arc lengths and uncertainties in *Gaia* and VLBI position estimates. Fig. 3 demonstrate that the *Gaia* position errors dominate over VLBI positions in normalized arc lengths. In particular, the median $\sigma_{v, \text{maj}}$ of the matches is 0.50 mas, while the median $\sigma_{g, \text{maj}}$ is 2.15 mas (compare with 2.3 mas for the total *Gaia* DR1 sample), i.e. a factor of 4 greater. The shape of the distribution remains non-Rayleighian even when we preform analysis of *Gaia* DR1 and VLBI rfc_2016c solutions among 2088 matches of the QS sample. Therefore, we conclude that the shape of the distribution is due to a peculiarity of the *Gaia* DR1 secondary solution errors that did not affect strongly the *Gaia* quasar auxiliary solution.

It is important to note that proper motions and parallaxes were estimated in the *Gaia* secondary solution. Since the time span of the data set used in producing the *Gaia* DR1 solution, 14 months, in general, is not sufficient for providing good estimates of parallax and proper motions, constraints were applied. The reciprocal weights of constraints were adjusted to make realistic errors of positions and parallaxes of stars (Michalik et al. 2015) that do have proper motions and parallaxes. This disfavoured treatment of AGNs that have negligible parallaxes and proper motion. Estimating proper motions and parallaxes in addition to the positions of AGNs inflated their formal uncertainties. See Michalik et al. (2015) for further details.

In order to check this hypothesis, we examined the parameter called the number of good observations along scan direction (NgAL) provided in the *Gaia* catalogue. NgAL varies from 2 to 1875 among the matches with the median value of 80. This parameter is proportional to the number of view crossings. We split the sample of matches into two equal sub-samples with NgAL below and above the median. The distributions among these sub-samples are indeed very different (Fig. 4). The distribution in the sub-sample with $\text{NgAL} \geq \text{median}$ fits reasonably well to the Rayleigh distribution with $\sigma = 1.38$, but the sub-sample with $\text{NgAL} < \text{median}$ does not. This confirms our conjecture that estimation of parallaxes and proper motions is responsible for inflation of the reported uncertainties.

We sought for a simple smooth function close to the Rayleigh distribution that can approximate the empirical distribution of normalized arc lengths. Our further analysis showed that the distribution has different shape for small and large *Gaia* position uncertainties. We found that the distribution of normalized arc lengths q of the sub-samples with *Gaia* semimajor error axes shorter and longer 5 mas can be represented as the Rayleigh distributions with differ-

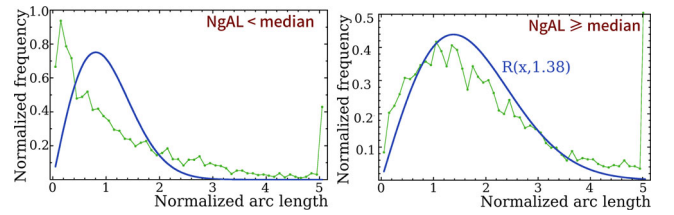


Figure 4. Normalized arc length distributions. Left: the sub-sample of 3001 matches with the number of good observations along scan below the median value 80. Right: the same for the sub-sample of 3054 matches with the number of good observations along scan at or above the median. The thick blue line shows the best fit to the Rayleigh distribution with parameter $\sigma = 1.38$.

Table 1. Parameters of the empirical model of normalized arc VLBI/*Gaia* for two ranges *Gaia* semimajor error axes. The second column shows the best fit to the power transformation parameter. The third column shows the scaling parameter of the best fit to the Rayleigh distribution after the power transformation. The last column shows the root mean square (rms) of residuals after fitting.

Range	λ	σ	rms
<5 mas	0.829	1.220	0.017
≥ 5 mas	0.465	0.622	0.158

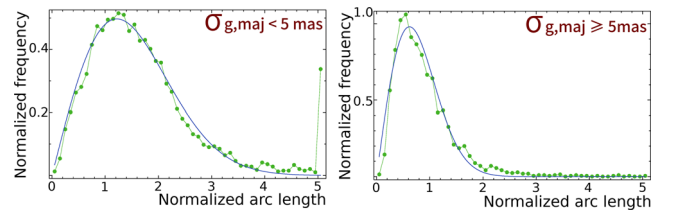


Figure 5. Left: the distribution of normalized arc lengths among VLBI/*Gaia* matches with $\sigma_{g, \text{maj}} < 5$ mas after the power transformation $\lambda = 0.829$. The blue line shows the best fit of the Rayleigh distribution with $\sigma = 1.240$ to the transformed distribution. Right: similar distribution among VLBI/*Gaia* matches with $\sigma_{g, \text{maj}} \geq 5$ mas after the power distribution $\lambda = 0.465$. The blue line shows the best fit of the Rayleigh distribution with $\sigma = 0.622$ to the transformed distribution.

ent scale parameters after applying the power-law transformation q^λ with different power parameters. The Table 1 shows parameters of the transformation and Fig. 5 illustrates the distributions of two sub-samples after the power-law transformation and their best fit to the Rayleigh distributions.

We split the matches into the bulk subset whose distribution obeys the power-law Rayleigh functions and a subset of matches with the probability to belong to the bulk subset below some threshold, i.e. outliers. We consider the offsets from the bulk subset are due to the random noise.

Since the probability $P(x > x_0) = e^{-\frac{x_0^2}{2\sigma^2}}$ for the Rayleigh distribution, we compute the probability for a given source to have the normalized power-law scaled arc length q^λ equal or greater than a given value due to the random noise as $P(q^\lambda) = e^{-\frac{q^{2\lambda}}{2\sigma^2}}$, where σ and λ are parameters from Table 1.

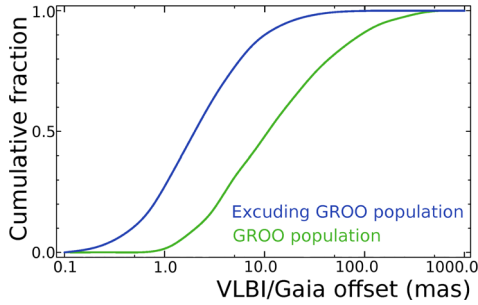


Figure 6. Cumulative distribution function of VLBI/*Gaia* offsets in logarithmic scale: green (lower) curve for the GROO population and blue (upper) curve for remaining sources.

4 SOURCES WITH STATISTICALLY SIGNIFICANT OFFSETS

We consider an offset between VLBI and *Gaia* positions statistically significant if both the PFA is less than 0.0002 and the probability that the position offset is caused by the random noise probability (RNP) is less than 0.01. There are 384 matches (6 per cent) that satisfy these criteria. See their cumulative distribution in Fig. 6. Table 2 shows these sources. Table 3 with remaining 5671 matches with $\text{PFA} < 0.0002$ and $\text{RNP} \geq 0.01$ is given in the electronic attachment only. It should be noted that the share of outliers among matches with the *Gaia* DR1 solution is very close to the share of outliers with the *Gaia* auxiliary quasar solution (also 6 per cent).

A number of reasons may result in statistically significant offsets: (1) errors in *Gaia* positions; (2) errors in VLBI positions; (3) GROO. We will consider both *Gaia* and VLBI errors that led to significant offsets as failures of quality control rather than random errors. We investigated which objects are more common among the sources with statistically significant offsets and found three groups: (1) sources with $\sigma_{v, \text{maj}} > 5$ mas (a factor of 1.9 more common); (2) sources brighter 17 mag (a factor of 2.7); and (3) sources with $\sigma_{g, \text{maj}} < 0.3$ mas (a factor of 1.6). The dominance of sources with position uncertainties greater than 5 mas indicates a possible failure of the quality control of VLBI data analysis for some sources in that group. Position uncertainties greater than 5 mas are usually obtained when a source was close to the detection limit and too few observations were collected. The weaker the signal-to-noise ratio, the more chances that a wrong maximum in the delay resolution function will be selected. Errors in group delay that correspond to the wrong maximum are significantly greater than their formal uncertainty computed assuming a correct maximum was found. The fewer observations, the more chances that a failure in fringe fitting will remain undetected. During past iterations of VLBI data analysis, a number of group delay estimates that correspond to an incorrect maximum in the delay resolution function were identified and fixed, which resulted in a change of source coordinate esti-

mates. It is conceivable that not all such observations have been identified and eliminated. But such oversights in quality control affects noticeably only positions of sources with too few observations, usually less than 20. The share of sources with 40 or less VLBI observations is 36 per cent among the objects with statistically significant offsets. That means that more than two-third matches with significant offsets cannot be affected by oversights in VLBI quality control.

A greater share of optically bright sources with small *Gaia* position errors favours a hypothesis that at least a part of objects with significant radio-optic offsets are GROO: smaller position uncertainties make position offsets statistically more significant if they are real.

Analysis of the group of sources with statistically significant offsets revealed there several gravitation lenses and a number of optically bright galaxies, but did not show any outstanding features that singles out these objects. The evidence collected so far supports the presence of the GROO population since observed significant radio/optic offsets cannot be explained only by failures in quality control. In order to explain the phenomenon of GROO, additional information should be examined. Kovalev, Petrov & Plavin (2017) investigated a connection between directions of AGN jets and offset directions. More studies focused on explanation of the GROO population are anticipated in the future.

5 SUMMARY

We explored offsets between *Gaia* DR1 and VLBI positions. We used the secondary data set for optical positions and recent VLBI solution rfc_2016c based on analysis of all available observations suitable for absolute astrometry collected since 1980 through 2016 July. We have found 6055 matched AGNs using the criterion set on their arc lengths, such that the mathematical expectation of the number of spurious matches in this sample is less than one object. When we used the *Gaia* auxiliary quasar solution, we were able to reproduce closely results of Mignard et al. (2016).

Comparison of *Gaia* DR1 and VLBI solutions revealed the following.

- (i) The median position offset is 2.2 mas – very close to the median semimajor axis of the error ellipse of *Gaia* positions in the entire data set.
- (ii) The median semimajor axis of the error ellipse of *Gaia* positions among the matches, 2.1 mas, is a factor of 4 greater than the median semimajor axis of the error ellipse of VLBI positions.
- (iii) The distribution of normalized arc lengths is significantly non-Rayleighian. We found evidence that the analysis strategy implemented in *Gaia* DR1 disfavoured sources with negligible parallaxes and proper motions, which inflated their uncertainties.
- (iv) There exists a population of sources with offsets statistically significant at the 99 per cent confidence level (6 per cent of the

Table 2. The first four rows of the table of 384 VLBI/*Gaia* matches with statistically significant offsets: probability of false association (PFA) less than 0.0002 and the random noise probability (RNP) less than 0.01. The fifth column contains the normalized arc lengths, and two last columns contain positions of *Gaia* minus VLBI over right ascensions, including $\cos \delta$ factor and declination. The full table is available in the electronic attachment.

VLBI ID	<i>Gaia</i> ID	PFA	RNP	q	d_α (mas)	d_δ (mas)
RFC J0000–3221	<i>Gaia</i> 2314315845817748992	4.47×10^{-8}	2.47×10^{-22}	20.78	– 6.51	– 0.83
RFC J0004–0802	<i>Gaia</i> 2441584492826114432	3.58×10^{-6}	4.14×10^{-03}	4.73	– 21.39	– 14.39
RFC J0005+3820	<i>Gaia</i> 2880735411259458048	1.98×10^{-7}	5.03×10^{-08}	10.80	5.77	– 3.43
RFC J0008–2339	<i>Gaia</i> 2337107759788510464	2.01×10^{-8}	5.84×10^{-06}	8.84	1.17	– 3.88
...						

matches). We admit that some these objects may have statistically significant offset due to failures in quality control in both VLBI and *Gaia* but certainly, not all: at maximum one-third. An increased share of optically bright objects with small position uncertainties in this population suggests that some these objects have GROO.

The emission centre in optic and in radio may not always coincide for a number of reasons. First, the centroid of the core may be shifted with frequency (e.g. Lobanov 1998; Kovalev et al. 2008). Secondly, unaccounted radio structure may cause an offset of the reference point with respect to the jet base, although such a shift is usually below 1 mas. Thirdly, as Condon et al. (2017) shown, there exist interacting galaxies within an optically weaker component hosting a bright radio source. In the era of ground optical astrometry, a study of such objects was limited to pairs at least 1 arcsec apart. *Gaia* astrometry has a potential to find such objects separated at milliarcsecond level. Finally, the presence of bright components along the jet may shift the optic centroid. At the moment, little is known about properties of jets at milliarcsecond scales in optic wavelengths. Investigation of the GROO population opens a new window into study of AGNs.

We should stress that this analysis is based on *Gaia* DR1 secondary data set and we expect statistics of comparison VLBI positions and future *Gaia* releases will be significantly different because of anticipated changes in data analysis strategy of *Gaia* observations.

ACKNOWLEDGEMENTS

It is our pleasure to thank Alexey Butkevich, Sergei Klioner, Alexandr Plavin and Eduardo Ros for fruitful discussions. We are very grateful to Lennart Lindegren for a detailed referee report and suggestions that helped us greatly to improve the manuscript and fix an error in numerical tables. This work is supported by the Russian Science Foundation grant 16–12–10481.

REFERENCES

- Beasley A. J., Gordon D., Peck A. B., Petrov L., MacMillan D. S., Fomalont E. B., Ma C., 2002, *ApJS*, 141, 13
 Condon J. J., Darling J., Kovalev Y. Y., Petrov L., 2017, *ApJ*, 834, 184
 Fey A. L. et al., 2015, *AJ*, 150, 58
 Fomalont E. B., Petrov L., MacMillan D. S., Gordon D., Ma C., 2003, *AJ*, 126, 2562
 Gordon D. et al., 2016, *AJ*, 151, 154
 Immer K. et al., 2011, *ApJS*, 194, 25
 Kovalev Y. Y., Petrov L., Fomalont E. B., Gordon D., 2007, *AJ*, 133, 1236
 Kovalev Y. Y., Lobanov A. P., Pushkarev A. B., Zensus J. A., 2008, *A&A*, 483, 759
 Kovalev Y. Y., Petrov L., Plavin A. V., 2017, *A&A*, 598, L1
 Lindegren L. et al., 2016, *A&A*, 595, A4

- Lobanov A., 1998, *A&A*, 330, A79
 Ma C. et al., 1998, *AJ*, 116, 516
 Michalik D., Lindegren L., Hobbs D., Butkevich A. G., 2015, *A&A*, 583, A68
 Mignard F. et al., 2016, *A&A*, 595, A5
 Orosz G., Frey S., 2013, *A&A*, 553, A13
 Petrov L., 2011, *AJ*, 142, 105
 Petrov L., 2012, *MNRAS*, 419, 1097
 Petrov L., 2013, *AJ*, 146, 5
 Petrov L., 2016, preprint (arXiv:1610.04951)
 Petrov L., Taylor G. B., 2011, *AJ*, 142, 89
 Petrov L., Kovalev Y. Y., Fomalont E. B., Gordon D., 2005, *AJ*, 129, 1163
 Petrov L., Kovalev Y. Y., Fomalont E. B., Gordon D., 2006, *AJ*, 131, 1872
 Petrov L., Kovalev Y. Y., Fomalont E. B., Gordon D., 2008, *AJ*, 136, 580
 Petrov L., Gordon D., Gipson J., MacMillan D., Ma C., Fomalont E., Walker R. C., Carabjal C., 2009, *J. Geod.*, 83, 859
 Petrov L., Kovalev Y. Y., Fomalont E. B., Gordon D., 2011a, *AJ*, 142, 35
 Petrov L., Phillips C., Bertarini A., Murphy T., Sadler E. M., 2011b, *MNRAS*, 414, 2528
 Schinzel F. K., Petrov L., Taylor G. B., Mahony E. K., Edwards P. G., Kovalev Y. Y., 2015, *ApJS*, 217, 4
 Shu F., Petrov L., Jiang W., McCallum J., Yi S.-O., Takefuji K., Li J., Lovell J., 2016, preprint (arXiv:1605.07036)
 Zacharias N., Zacharias M. I., 2014, *AJ*, 147, 95
 Zacharias N., Monet D. G., Levine S. E., Urban S. E., Gaume R., Wycoff G. L., 2004, *Bull. Am. Astron. Soc.*, 36, 1418

SUPPORTING INFORMATION

Supplementary data are available at *MNRASL* online.

Table 2. 384 VLBI/*Gaia* matches with statistically significant offsets: probability of false association (PFA) less than 0.0002 and the random noise probability (RNP) less than 0.01. The fifth column contains the normalized arc lengths, and two last columns contain positions of *Gaia* minus VLBI over right ascensions, including $\cos \delta$ factor and declination.

Table 3. 5671 VLBI/*Gaia* matches with statistically significant off-Q sets: probability of false association (PFA) less than 0.0002 and the random noise probability (RNP) is equal or greater than 0.01. The fifth column contains the normalized arc lengths, and two last columns contain positions of *Gaia* minus VLBI over right ascensions, including $\cos \delta$ factor and declination.

Please note: Oxford University Press is not responsible for the content or functionality of any supporting materials supplied by the authors. Any queries (other than missing material) should be directed to the corresponding author for the article.

This paper has been typeset from a $\text{\TeX}/\text{\LaTeX}$ file prepared by the author.